Journal of Metals, Materials and Minerals, Vol.28 No.2 pp.18-26, 2018

Phase separation dynamics and morphologies prediction of PEO-b-PMMA copolymer by atomistic and mesoscopic simulations

Natthiti CHIANGRAENG[1,2], Vannajan S. LEE[3], and Piyarat NIMMANPIPUG[1,*]

[1]*Department of Chemistry, Faculty of Science, Chiang Mai University, Chiang Mai 50200, Thailand*
[2]*Doctor of Philosophy Program in Chemistry, Faculty of Science, Chiang Mai University, Chiang Mai 50200, Thailand*
[3]*Department of Chemistry, Faculty of Science, University of Malaya, Kuala Lumpur 50603, Malaysia*

***Corresponding author e-mail:** piyarat.n@cmu.ac.th

Received date:
7 May 2018
Revised date:
30 August 2018
Accepted date:
31 August 2018

Keywords:
Morphologies
Phase separation
Block copolymers
Free Energy Density
Order Parameter

Abstract

Atomistic and mesoscopic simulations are the most important tools to predict the morphologies of block copolymers. In this study, inter-bead interactions and essential parameters for meso-structure polymeric models were optimized for poly(ethylene oxide)-block-poly(methyl methacrylate) (PEO-b-PMMA; O-b-M) binary systems. A coarse-grained model in a mesoscopic dynamic was used to represent polymeric chain. Gaussian chain is calculated from polymer chain length concerning its characteristic properties. Free energy density was considered by setting suitable time steps and inter-bead interactions for meso-structure simulations. The interaction energies of 1:1, 2:1 and 4:1 molar ratio of O to M segments were 3.67, 4.66, and 5.92, respectively. These values are obtained from Flory-Huggins parameters in atomistic simulations. Morphology at equilibrium was obtained in five different types: worm-like micelle, defected lamellar, lamellar, spherical micelle and bicontinuous at 400 K from M5-1M2-O5, O4-O4M6, M4-M5O5, O10-2M122-O10 and M11-1M2-O10, respectively. The obtained morphologies correlate with order parameter developed from the simulations.

1. Introduction

Block copolymers (BCPs) are interesting materials in the plastic industry as they can present tuneable microstructure, thermal and mechanical properties [1-3]. Morphology of BCPs depends on various factors including temperature which is used to control the obtained structure in the manufacturing [4,5]. Various self-assembly of BCPs provides nanoscale patterning possibility and have been extensively studied due to their unique chain architecture and physical properties [6-8].

Poly(ethylene oxide), PEO and poly(methyl methacrylate), PMMA are biocompatible materials and biomedical polymers with different hydrophilicity. PEO is a flexible and non-toxic polymer [9-11]. It has been used in many commercial applications by vary their molecular weight such as packaging and moisture barrier film [12]. PEO and PMMA copolymers have been widely applied in engineering field and synthesized amphiphilic graft copolymers for drug carriers [13]. It is well known that PEO and PMMA have a weak interaction between polymeric chains. They are quite immiscible in molten and solid state [14,15]. Although synthesis and characterization of amphiphilic copolymers composed of PMMA and PEO and compatibility of PEO/PMMA blends have been broadly investigated, there is still limited report about self-assembling properties of PMMA-PEO block copolymers. To predict miscibility between PEO and PMMA, the Flory-Huggins parameter, χ is considered. χ can be obtained from some experimental methods, including solvent diffusion, and inverse gas chromatography.

Numbers of modelling and simulations have been carried out for fitting the required parameters to properties of polymer compatibility. The blending between poly(vinyl alcohol), PVA and PMMA was studied by atomistic and mesoscopic simulations. The results shown the order parameter of the polymer blend is less than 0.1 when PVA composition is more than 60 wt%, the blend is miscible. The experimental differential scanning calorimetry data supported this observation [16]. Mu *et al.* [17] studied polystyrene, PS and PMMA blends by atomistic and mesoscopic simulations. They found few ways to enhance the compatibility

DOI: 10.14456/jmmm.2018.21

of these polymer blends. The first one is addition of a block copolymer which consisting of PS and PMMA on phase morphology. The same composition between added block copolymer and a blend were linked together. This way can induce the compatibility of the blend, especially adding the block copolymer with high PS composition. In addition, applied the shear stress and added the nanoparticle are others way to enhance the compatibility. This effect not only depends on types of factor were used but they also depend on their composition.

In this work, inter-bead interaction and essential parameters were analysed from the six poly(ethylene oxide)-block-poly(methyl methacrylate) (PEO-b-PMMA; O-b-M) models to predict the morphologies of BCPs. Atomistic and mesoscopic simulations were employed to study phase separation dynamics correlating with morphologies. The order parameter and free energy density values which are important parameter to examine the phase behaviour were considered.

2. Experimental

This paper consists of two calculation steps; atomistic and mesoscopic simulations. In this study, all simulations were performed using Materials Studio software package version 5.5 (Accelrys) [18]. The Flory-Huggins parameter is an intermediate parameter for connecting between the microscale and mesoscale. In this study, the morphologies of copolymer that consists of poly(ethylene oxide), -CH_2CH_2O-, and poly(methyl methacrylate), -$CH_2C(CH_3)(COOCH_3)$-, will be carried out. In this research, six architectures which were M_5-1M2-O_5, O4-O_4M_6, M4-M_5O_5, O_{10}-2M_{12}2-O_{10}, M_{11}-1M2-O_{10} and O_5-2$M_6$2-O_5 were investigated. O and M represent poly(ethylene oxide) and poly(methyl methacrylate), respectively. These models represented branch architectures will be defined in as in mesoscopic simulations. The branch architectures had different arm and length. Effects of arm number, chain length as well as an arrangement of polymers will be analysed and discussed in this study.

2.1 Atomistic simulations

The solubility parameters of both pure and mixed polymers were calculated by atomistic simulations. The COMPASS [19] (condensed-phase optimized molecular potentials for the atomistic simulation studies) force field was used in the interatomic interaction calculations. In general, the COMPASS force field is an appropriate choice to calculate solubility parameter which correlates with cohesive energy density value, particularly, for polymeric systems. The total energy (E_T) of system was considered as summation of bonded and non-bonded interactions as follows.

$$E_T = E_b + E_o + E_\Phi + E_{oop} + E_{pe} + E_{vdw} + E_q \quad (1)$$

In above equation, the first five terms represent the bonded interactions, which corresponding to the bond (E_b), bond angle bending (E_o), torsion angle rotation (E_Φ), out of plane (E_{oop}), and potential energy (E_{pe}). The last two terms represent the non-bonded interaction, which consisting of the van der Waals interaction (E_{vdw}), and electrostatic force (E_q). In this force field, E_{vdw} was described by the Lennard-Jones 6-12 potential, while the electrostatic energy was calculated from the partial charges of atoms in the system, which estimated by the charge equilibrium method. Electrostatic interaction was calculated according to the Ewald summation method since it calculated long-range interaction more accurately.

The representative polymer chain length, RCL, is the same, 50 repeating unit, for both PEO and PMMA. The details of all initial systems are shown in Table 1. The molar ratio of PEO-PMMA for blend models, including the number of minimum representative polymer chain length per unit cell, the percentage of PEO weight, and its density are presented. 3 D atomistic models for these initial structures are shown in Figure 1.

Table 1. Initial conditions of PEO/PMMA models.

	Model	Composition	wt% of PEO	Density (g/cm^3) [20]
I	Pure PMMA	1PMMA	0	1.188
II	1/1	1PEO, 1PMMA	30.6	1.1849
III	2/1	2PEO, 1PMMA	46.8	1.1833
IV	4/1	4PEO, 1PMMA	63.8	1.1816
V	Pure PEO	1PEO	100	1.178
VI	Pure PEO	2PEO	100	1.178
VII	Pure PEO	4PEO	100	1.178

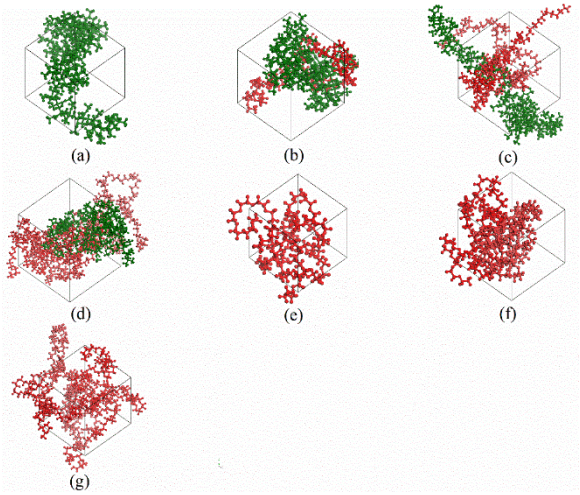

Figure 1. Initial structure of seven models (a) model I: 1PMMA (b) model II: 1PEO, 1PMMA (c) model III: 2PEO, 1PMMA (d) model IV: 4PEO, 1PMMA (e) model V: 1PEO (f) model VI: 2PEO and (g) model VII: 4PEO. Red represents the PEO chain(s) and Green represents the PMMA chain.

Each system was minimized by using the conjugate gradient method with energy convergence limit of 1.0×10^{-6} kcal/ mol. The minimized configurations were relaxed under constant temperature and density by NVT ensemble molecular dynamics (MD) simulation for 200 ps. A time step of 1 fs was used to ensure the stability of simulation and the temperature was controlled by Anderson thermostat at 400 K where PMMA-b-PEO can be found in a two-phase regime [21]. Next, polymer chains were annealed at temperature range from 270 K to 320 K and from 370 K to 440 K for PEO and PMMA systems, respectively [22,23]. The duration for each annealing cycle is set at 10 ns. The lower and upper temperature is the value between glass transition temperature, T_g and crystalline melting temperature, T_m of each polymer respectively. Then, to reduce the end- to- end interactions of the polymer, MD simulations under constant temperature and pressure (NPT ensemble) were carried out for 200 ps, this process was repeated for three times. Finally, the equilibrium configurations were obtained by MD simulations with NVT ensemble for 100 ps to collect data.

2.2 Mesoscopic simulations

Mesoscopic dynamics simulation was used to predict polymeric morphology. Gaussian chain is calculated from polymer chain length concerning its characteristic properties; characteristic ratio (C_∞). Each bead is a representative of the polymer with the length equivalent to statistical segments.

There are two sets of essential parameters for morphologies predictions in mesoscopic dynamics simulation: There are a molecular topology which described by beads and interaction energies. The coarse-grained model of PEO and PMMA could be designed from its minimum representative polymer chain length as a repeating unit and characteristic ratio of polymers. The characteristic ratio of PEO and PMMA are 9.89 and 8.65, respectively, and the minimum representative polymer chain length of PEO and PMMA are 50 repeating units. For PEO, the coarse-grained length of PEO is 5 units for the minimum representative polymer chain length. In the same way, the coarse-grained length of PMMA is 6. Accordingly, the atomistic chain of the polymer PEO_{50} and $PMMA_{50}$ was projected to model O_5 and M_6.

Six different coarse-grained models of PEO-b-PMMA copolymers were designed: O4-O_4M_6, M4-M_5O_5, M_5-1M2-O_5, O_5-2$M_6$2-O_5, M_{11}-1M2-O_{10}, and O_{10}-2M_{12}2-O_{10}, their O to M segments ratio are 1:1, 1:1, 2:1, 4:1, 2:1 and 4:1 respectively. The code name for these block copolymers were separated in two parts. For the first part, the letter demonstrates the polymer bead type of branched point; O for ethylene oxide and M for methyl methacrylate. The subscript number is number of bead for each polymer segment and the in-line number indicates the arm number for each branched point. The next part is branched point and it is located after and/or before the hyphen symbol. Taking M_5-1M2-O_5 as an example, this block copolymer has a methyl methacrylate as branched point. It consists of three branches from a methyl methacrylate. One is a methyl methacrylate which each branch consists of five beads and other branches are ethylene oxide chains consisting of five beads. The schematic illustration of coarse grain models was shown in Figure 2.

All simulations were performed at 400 K. The grid dimensions were taken as $32 \times 32 \times 32$ nm^3 with the grid spacing of 1.0 nm and the bond length was 1.1543 nm. A bead diffusion coefficient was set as 1.0×10^{-7}cm^{2}s^{-1}. The total simulation time is 2.5 ms and the number of step is 50000 steps. The constant noise-scaling parameter of 100 and the compressibility parameter of 10.0 were chosen in this simulation.

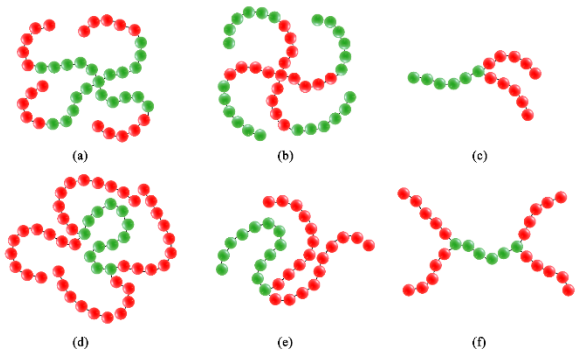

Figure 2. Coarse grain models of (a) M4-M_5O_5 (b) O4-O_4M_6 (c) M_5-1M2-O_5 (d) O_{10}-2M_{12}2-O_{10} (e) M_{11}-1M2-O_{10} and (f) O_5-2$M_6$2-O_5, Red bead represents the PEO and Green bead represents the PMMA.

3. Results and discussion

3.1 Atomistic simulations

In this study, the binary systems consist of the PEO and PMMA. The density of PEO and that of PMMA are 1.178 g/cm^3 and 1.188 g/cm^3 was set for atomistic simulations. The density of the mixed polymer depends on the molar ratio of system and correlate with number of polymer in the simulation box.

The solubility parameters (δ) of the mixed and pure components can be used to calculate the cohesive energy density (*CED*). The relation between them follows the equation:

$$CED = \frac{E_{\text{coh}}}{V} = \delta^2 \qquad (2)$$

The assembly of each binary polymer chain depends on the cohesive energy density of each system. The different composition component will result in different cohesive energy density. Cohesive energy from both mixed and pure components were applied to calculate the Flory-Huggins parameter, χ as shown below:

$$\chi = \left(\frac{\Delta E_{\text{mix}}}{RT}\right) V_{mon} \qquad (3)$$

where, V_{mon} is the unit volume of one monomer. For this blends of PEO and PMMA, V_{mon} of one monomer equals 140 cm^3/mol. Then, ΔE_{mix} of the mixing binary blends can be obtained by:

$$\Delta E_{\text{mix}} = \phi_{\text{O}} \left(\frac{E_{\text{coh}}}{V}\right)_{\text{pure}} + \phi_{\text{M}} \left(\frac{E_{coh}}{V}\right)_{\text{pure}} - \left(\frac{E_{coh}}{V}\right)_{\text{mixed}} \qquad (4)$$

Where, ϕ is a volume fraction of each polymer, the subscripts O and M represent PEO and PMMA, respectively. The subscripts pure and mixed demonstrate the cohesive energy density of pure components and the mixing for binary mixture, respectively. The cohesive energy per volume or the *CED* of PEO, PMMA and the mixing binary systems are presented in Table 2. For example, M_5-1M2- O_5 and M_{11}- 1M2- O_{10} had a molar ratio between PEO and PMMA of 2: 1; three systems were used to calculate the energy of mixing, including system number I, III and VI which represented the system of pure PMMA, the mixing of PEO and PMMA with a molar ratio between PEO and PMMA of 2:1, and pure PEO, respectively. The interaction energies of the various bead types (ε_{OM}) calculated from the Flory-Huggins parameter, χ at 400 K were shown in Table 3. A positive value of ε_{OM} parameter indicates a repulsion interaction between O and M beads. On the other hand, the interaction energy between the same species is all 0 ($\varepsilon_{\text{MM}} = 0$, $\varepsilon_{\text{OO}} = 0$).

Table 2. *CED* of PEO, PMMA and the mixing binary systems.

Number of RCL		δ	*CED* × 10^{-7}
PEO	PMMA	(cal/cm^3)$^{0.5}$	(cal/m^3)
0	1	6.44021	4.14763
1	1	8.68708	7.54654
2	1	8.56458	7.33520
4	1	8.71396	7.59331
1	0	8.40341	7.06173
2	0	8.37415	7.01264
4	0	9.60658	9.22865

Table 3. The interaction energies of the various bead types (ε_{OM}).

Ratio of O to M segments	ε_{OM}
1:1	3.67
2:1	4.66
4:1	5.92

To understand whether both PEO and PMMA are miscible or immiscible, a critical value of χ, ($\chi_{\text{OM, critical}}$) should be calculated by the following equation:

$$\chi_{\text{OM}} = \frac{1}{2}\left(\frac{1}{\sqrt{m_{\text{O}}}} + \frac{1}{\sqrt{m_{\text{M}}}}\right)^2 \qquad (5)$$

Where, m_{O} and m_{M} represent the degree of polymerization of O and M of representative polymer chain length. There is existent number of repeating unit or the number of representative polymer chain length which obtained from atomistic simulation. The critical values of χ are based on the same reference volume. According to this equation, it can be used to indicate the compatibility or incompatibility of the blends. In general, the blends are miscible if ($\chi_{\text{OM, calculated}}$) <

($\chi_{OM,\ critical}$). For this case, the Gibbs free energy (ΔG_m) is negative. On the other hand, if ($\chi_{OM,\ calculated}$) $\gg$ ($\chi_{OM,\ critical}$), the blends are immiscible. So, they form two separated phases. In the last case, if ($\chi_{OM,\ calculated}$) and ($\chi_{OM,\ critical}$) are small difference, the blends are partially miscible. In our studies, PEO and PMMA blends, we calculated the ($\chi_{OM,\ calculated}$) of 1:1, 2:1 and 4:1 molar ratio is 0.00221, 0.00280, and 0.00356, respectively. The ($\chi_{OM,\ critical}$) of PEO and PMMA blends is 0.04, which is much higher than the calculated ($\chi_{OM,\ calculated}$) values. Therefore, it is indicated that the PEO and PMMA blends are miscible at 400 K.

3.2 Mesoscopic simulations

Mesoscopic simulation was used to investigate the phase separation dynamic of PEO/ PMMA systems. In Mesoscopic Dynamics (MesoDyn) simulation, there are two essential parameters for a simulation to predict the morphologies. The first parameter is a coarse-grained length chain, called Gaussian chain. It was used to determine the polymeric chain of each polymer. Another parameter is the interaction energies. This parameter can be calculated through this equation:

$$V^{-1}\varepsilon_{ij} = \chi_{ij}RT \qquad (6)$$

Where, χ_{ij}, the Flory-Huggins parameter, was taken from previous atomistic simulation results of PEO/PMMA blends using a different composition, R is the molar gas constant (8.314 J/mol·K) and T is simulation temperature kept at 400 K.

The order parameter (P_I) is the mean squared deviation from homogeneity in volume V. It is defined as the average volume of the difference between the local density squares and the overall density squared following equation:

$$P_I = \frac{1}{V}\int_V \left[\eta_I^2(r) - \eta_I^2\right] dr \qquad (7)$$

where, η_I is dimensionless density (volume fraction) for species I. The larger the value of order parameter is the stronger the phase separation. The small value of order parameter indicates a mixed state, which is a better compatibility or miscibility. In addition, the free energy density [24,25] can be a good index for evaluating the dynamic state. They should asymptotically approach a stable value as the system reaches dynamic equilibrium during the mesoscopic simulation. The free energy density is calculated based on the dynamic mean-field density functional theory. Therefore, this density is no routinely calculated for real systems, and it is not possible to directly compare with experimental free energy data [26].

Order parameter value and free energy density value (RT/volume) are shown in Figure 3. It can be seen that the dynamic evolution of mesostructured can confirmed by both the order parameter and free energy density values over time. In the initial state, the morphology is homogeneous with low order parameter. Then, the order parameters gradually increase while the free energy density value decreases over time. After 950 μs, both the order parameter and the free energy density are mostly constant. It is indicating that the system has arrived the dynamic equilibrium state. In this state, the equilibrium morphology of each system was obtained. As order parameters gradually increased to approximately 950 μs, the morphology slowly changed into phase separation. However, the phase change was not significantly observed until 550 μs. The phase change was observed between 550 to 950 μs and no phase changing was observed after 950 μs.

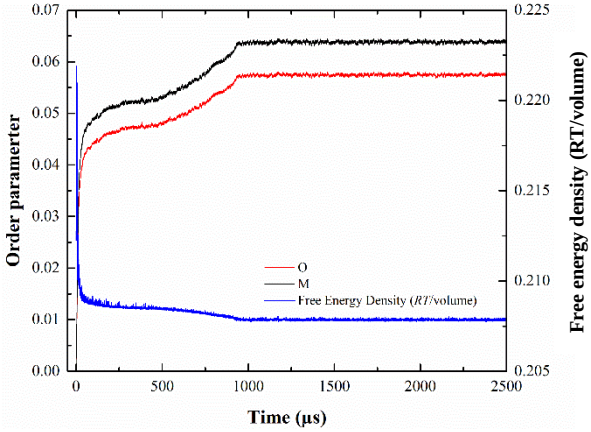

Figure 3. Order parameter and free energy density during the meso-phase formation of M4-M_5O_5 BCP over time.

In this study, phase separation was observed in agreement with experiment investigations [14,27] and previous simulation study [20]. Six different mesoscopic structures were obtained as shown in Figure 4. The morphology at equilibrium state of phase separation was obtained in five types: worm-like micelle, defected lamellar, lamellar, spherical micelle and bicontinuous for M_5-1M2-O_5, O4-O_4M_6, M4-M_5O_5, O_{10}-$2M_{12}2$-O_{10} and M_{11}-1M2-O_{10}, respectively. O_5-$2M_6$2-O_5 remains an unaltered phase morphology, the structure persists disorder.

In Figure 5 the evolution of the free energy density was shown. This parameter is used to indicate the equilibrium state of each morphology. In the initial state, the free energy density rapidly decreasing in the first 100 μs for worm- like micelle, lamellar, defected lamellar, spherical micelle, and bicontinuous without disorder phase. After that, it reaches equilibrium. From this state, the morphology of each structure was stable until the average of base line for the free energy density was changed again.

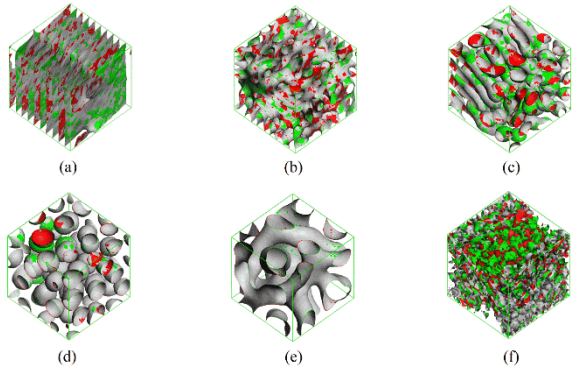

Figure 4. Meso-structures of PEO-b-PMMA BCPs of (a) lamellar (b) defected lamellar (c) worm-like micelle (d) spherical micelle (e) bicontinuous and (f) disorder phase. Red represents the O isosurface, green represents the M isosurface, and gray correspond to the interface between them.

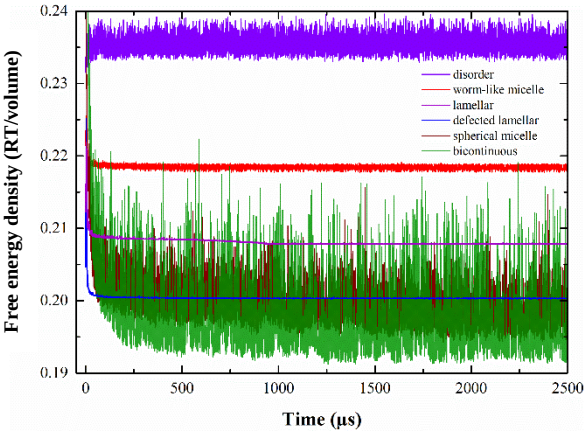

Figure 5. The evolution of the free energy density versus time (μs) of each morphology.

Disorder phase had a different trend of free energy density and it provided the highest free energy density value. On the other hands, bicontinuous structure provided the lowest free energy density value but the value which fluctuated around an average value at equilibrium state. Spherical micelle structure resembled structure showing a trend like bicontinuous structure, the value also fluctuated around an average value at its equilibrium state. Free energy density at equilibrium state of worm- like micelle, lamellar, and defected lamellar are quite stable.

To concretely consider the morphology at equilibrium state, order parameter of each system was considered together with free energy density. These two parameters can be used to confirm the morphology at equilibrium state. The trend of order parameter value and free energy density value are in opposite direction. The turning point of two parameters occur at the same time e.g. at 950 μs for lamellar structure. The evolution of the order parameter of each morphology over time was illustrated in Figure 6. It can be seen that disorder phase had the lowest order parameter of PEO and PMMA, it converges to zero. This lowest value indicates better compatibility or miscibility of system. The morphology is homogeneous, called disorder phase. On the other hand, bicontinuous structure had the highest order parameter of PEO and PMMA with the lowest free energy density while spherical micelle had a medium order parameter and the free energy density is low. So, this value indicates a strong phase separation for bicontinuous. The free energy densities of these two morphologies are in similar trend. The order parameters of lamellar, defected lamellar and worm- like micelle morphologies were nearly identical, and they located at low order parameter region.

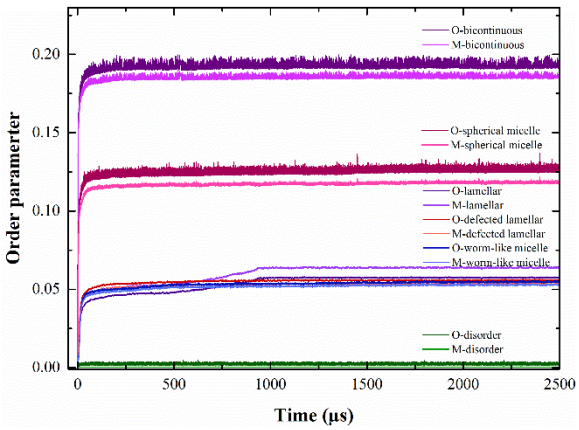

Figure 6. The evolution of the order parameter values versus time (μs) of each morphology.

In this study, lamellar, defected lamellar, and worm- like micelle structures were mainly discussed. The close- up evolution of the order parameter values for their structures over time as displayed in Figure 7. It can be seen that the trend

of defected lamellar and worm- like micelle structure are likely the same but they had different value over time. The order parameter values increased rapidly, it indicates that, the meso-structures can hardly change for less than 100 μs.

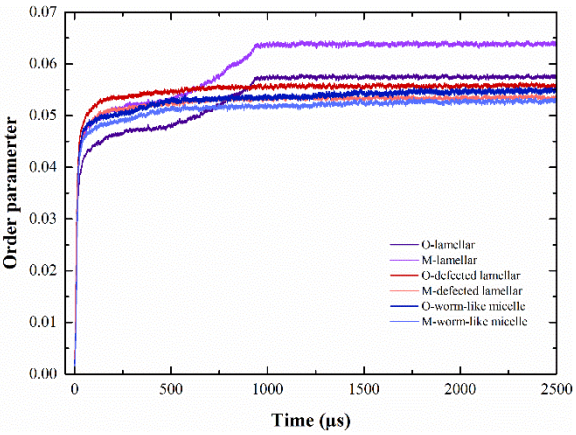

Figure 7. The close-up evolution of the order parameter versus time (μs) for lamellar, defected lamellar and worm-like micelle structures.

The evolution of the meso-structures for defected lamellar and worm-like micelle structures over time is shown in Figure 8- 9. For lamellar, defected lamellar and worm- like micelle cases, each structure is in disorder state in the first 5 μs. After that, the structure hardly changed the characteristic morphology which is mainly correlated with its architectural structure. Although the order parameter values were similar but the meso- structures were distinct due to the different of the architecture and interactions that make polymer chains are irregularly arranged in system. The stability of lamellar structures occurs over 950 μs. The evolution of the meso- structures for lamellar structures can be seen in Figure 10.

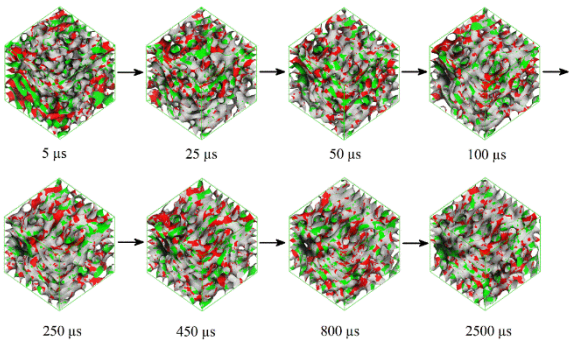

Figure 8. The evolution of the meso-structures versus time (μs) for defected lamellar structures.

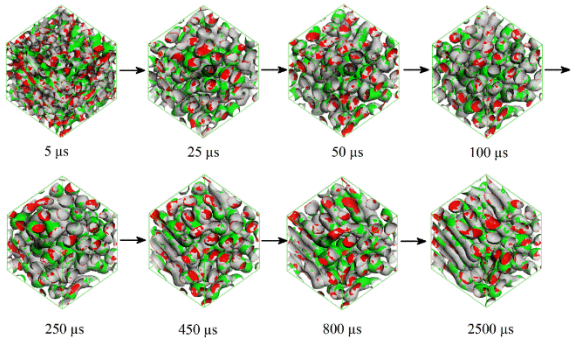

Figure 9. The evolution of the meso-structures versus time (μs) for worm-like micelle structures.

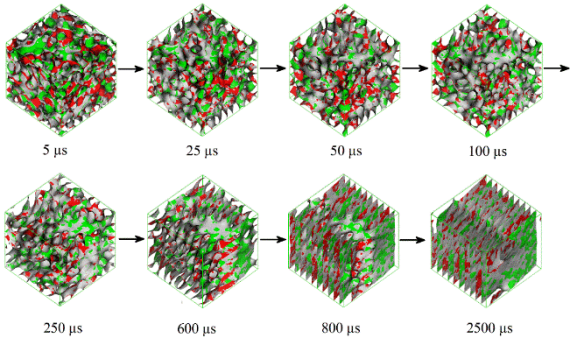

Figure 10. The evolution of the meso-structures versus time (μs) for lamellar structures.

4. Conclusions

The annealing process and MD simulations (NVT and NPT ensemble) are important process to reduce the end-end interactions between polymers. The solubility value of polymer in the simulated systems are close to the experimental data by setting suitable time steps and number of repeating unit. The Flory-Huggins parameter, χ can be calculated from solubility of each system. The calculated MesoDyn input parameter were carried out at 400 K and there were 3.67, 4.66, and 5.92 kJ/mol for 1: 1, 2: 1, and 4: 1 ratio of O to M segments, respectively. This parameter depends on ratio of O to M segments. For mesoscale simulations, morphology of each system at equilibrium was obtained in five types, including worm-like micelle, defected lamellar, lamellar, spherical micelle and bicontinuous at 400 K which were M_5-1M2-O_5, O4-O_4M_6, M4-M_5O_5, O_{10}-2M_{12}2-O_{10} and M_{11}-1M2-O_{10}, respectively which correlate with order parameter that get from the simulation. The morphology at equilibrium state can be confirmed by both the order parameter and free energy density values over time. When two parameters approach a

stable value, the system has achieved equilibrium state of morphology structure.

5. Acknowledgements

NC acknowledges resources from Computational Simulation and Modelling Laboratory (CSML), Chiang Mai University (CMU) and scholarship from Science Achievement Scholarship of Thailand (SAST). The authors acknowledge the National Nanotechnology Center for Material Studio software. The authors gratefully acknowledge the partial financial support from CMU-IC research project for Asean+3 Cross Border Research, the Center of Excellence for Innovation in Analytical Science, CMU and Standardization and Development of Miang Extract and Chemical Analysis Methodology Project, ARDA & NRCT, Thailand.

References

[1] M. Lazzari and M. A. López-Quintela, "Block copolymers as a tool for nanomaterial fabrication," *Advanced Materials*, vol. 15, pp. 1583-1594, 2003.

[2] C. Schatz and S. Lecommandoux, "Polysaccharide-containing block copolymers: synthesis, properties and applications of an emerging family of glycoconjugates," *Macromolecular Rapid Communications*, vol. 31, pp. 1664-1684, 2010.

[3] K. Yang and C. D. Han, "Effects of shear flow and annealing on the morphology of rapidly precipitated immiscible blends of polystyrene and polyisoprene," *Polymer*, vol. 37, pp. 5795-5805, 1996

[4] P. Bhargava, Y. Tu, J. X. Zheng, H. Xiong, R.P. Quirk and S. Z. D. Cheng, "Temperature-induced reversible morphological changes of polystyrene-block-poly(ethylene oxide) micelles in solution," *Journal of the American Chemical Society*, vol. 129, pp. 1113-1121, 2007.

[5] I. Barandiaran, D. Katsigiannopoulos, E. Grana, A. Avgeropoulos, A. Eceiza and G. Kortaberria, "PI-b-PMMA diblock copolymers: nanostructure development in thin films and nanostructuring of thermosetting epoxy systems," *Colloid and Polymer Science*, vol. 291, pp. 2173-2180, 2013.

[6] M. Park, C. Harrison, P. M. Chaikin, R. A. Register and D. H. Adamson, "Block copolymer lithography: periodic arrays of ~10^{11} holes in 1 square centimeter," *Science*, vol. 276, pp. 1401-1404, 1997.

[7] T. Thurn-Albrecht, R. Steiner, J. DeRouchey, C. M. Stafford, E. Huang, M. Bal, M. Tuominen, C. J. Hawker and T. P. Russell, "Nanoscopic templates from oriented block copolymer films," *Advanced Materials*, vol. 12, pp. 787-791, 2000.

[8] T. Thurn-Albrecht, J. Schotter, G. A. Kästle, N. Emley, T. Shibauchi, L. Krusin-Elbaum, K. Guarini, C. T. Black, M. T. Tuominen and T. P. Russell, "Ultrahigh-density nanowire arrays grown in self-assembled diblock copolymer templates," *Science*, vol. 290, pp. 2126-2129, 2000.

[9] J. H. Park, K. D. Park and Y. H. Bae, "PDMS-based polyurethanes with MPEG grafts: synthesis, characterization and platelet adhesion study," *Biomaterials*, vol. 20, pp. 943-953, 1999.

[10] K. Bergström, K. Holmberg, A. Safranj, A. S. Hoffman, M. J. Edgell, A. Kozlowski, B. A. Hovanes and J. M. Harris, "Reduction of fibrinogen adsorption on PEG-coated polystyrene surfaces," *Journal of Biomedical Materials Research*, vol. 26, pp. 779-790, 1992.

[11] S. Nagaoka and A. Nakao, "Clinical application of antithrombogenic hydrogel with long poly(ethylene oxide) chains," *Biomaterials*, vol. 11, pp. 119-121, 1990.

[12] F. B. Bailey and J. V. Koleske, *Poly(ethylene oxide)*. New York: Academic Press, 1976.

[13] H. -C. Chi, C. -S. Chern, C. -K. Lee and H. -F. Chang, "Synthesis and characterization of amphiphilic poly(ethylene glycol) graft copolymers and their potential application as drug carriers," *Polymer*, vol. 39, pp. 1609-1616, 1998.

[14] S. Schantz, "Structure and mobility in poly(ethylene oxide)/poly(methyl methacrylate) blends investigated by ^{13}C solid-state NMR," *Macromolecules*, vol. 30, pp. 1419-1425, 1997.

[15] J. A. Zawada, C. M. Ylitalo, G. G. Fuller, R. H. Colby and T. E. Long, "Component relaxation dynamics in a miscible polymer blend: poly(ethylene oxide)/poly(methyl methacrylate)," *Macromolecules*, vol. 25, pp. 2896-2902, 1992.

[16] S. S. Jawalkar, S. G. Adoor, M. Sairam, M. N. Nadagouda and T. M. Aminabhavi, "Molecular modeling on the binary blend compatibility of poly(vinyl alcohol) and poly(methyl methacrylate): an atomistic simulation and thermodynamic approach," *Journal of Physical Chemistry B*, vol. 109, pp. 15611-15620, 2005.

[17] D. Mu, J. -Q. Li and Y. -H. Zhou, "Modeling and analysis of the compatibility of polystyrene/poly(methyl methacrylate) blends with four inducing effects," *Journal of Molecular Modeling*, vol. 17, pp. 607-619, 2011.

[18] M. Studio, Accelrys Software Inc. 2011.

[19] S. S. Jawalkar, S. K. Nataraj, A. V. Raghu and T. M. Aminabhavi, "Molecular dynamics simulations on the blends of poly(vinyl pyrrolidone) and poly(bisphenol-A-ether sulfone)," *Journal of Applied Polymer Science*, vol. 108, pp. 3572-3576, 2008.

[20] D. Mu, X. -H. Huang, Z. -Y. Lu and C. Sun, "Computer simulation study on the compatibility of poly(ethylene oxide)/ poly(methyl methacrylate) blends," *Chemical Physics*, vol. 348, pp. 122-129, 2008.

[21] Y. Murakami, "Studies on compatibility of poly(ethylene oxide) and poly(methyl methacrylate) by inverse gas chromatography," *Polymer Journal*, vol. 220, pp. 549-556, 1988.

[22] J. E. Mark, *Polymer data handbook*. New York: Oxford University Press, Inc., 1999.

[23] E. Calahorra, M. Cortazar and G. M. Guzmán, "Thermal decomposition of poly(ethylene oxide), poly(methyl methacrylate), and their mixtures by thermogravimetric method," *Journal of Polymer Science: Polymer Letters Edition*, vol. 23, pp. 257-260, 1985.

[24] J. G. E. M. Fraaije, B. A. C. van Vimmeren, N. M. Maurits, M. Postma, O. A. Evers, C. Hoffmann, P. Altevogt and G. Goldbeck-Wood, "The dynamic mean-field density functional method and its application to the mesoscopic dynamics of quenched block copolymer melts," *Journal of Chemical Physics*, vol. 106, pp. 4260-4269, 1997.

[25] P. Altevogt, O. A. Evers, J. G. E M. Fraaije, N. M. Maurits and B. A. C. van Vlimmeren, "The MesoDyn project: software for mesoscale chemical engineering," *Journal of Molecular Structure: THEOCHEM*, vol. 463, pp. 139-143, 1999.

[26] S. S. Jawalkar and T. M. Aminabhavi, "Molecular modeling simulations and thermodynamic approaches to investigate compatibility/incompatibility of poly(l-lactide) and poly(vinyl alcohol) blends," *Polymer*, vol. 47, pp. 8061-8071, 2006.

[27] A. C. Fernandes, J. W. Barlow and D. R. Paul, "Blends containing polymers of epichlorohydrin and ethylene oxide. Part I: Polymethacrylates," *Journal of Applied Polymer Science*, vol. 32, pp. 5481-5508, 1986.